

Doi: 10.58414/SCIENTIFICTEMPER.2025.16.4.18

## **RESEARCH ARTICLE**

# Fractional thermoviscoelastic damping response in a non-simple micro-beam via DPL and KG nonlocality effect

Gulshan Makkad\*, Lalsingh Khalsa, Vinod Varghese

#### **Abstract**

This study introduces a novel framework for investigating thermoelastic damping (TED) in viscoelastic micro-scale rectangular beams using the Euler-Bernoulli beam theory (EBBT). A two-temperature thermoviscoelastic model is developed, uniquely integrating non-Fourier effects and fractional-order parameters through a generalized thermoelasticity approach with an internal heat source and the dual-phase-lag (DPL) thermal conduction model. This innovative approach addresses the limitations of classical models by incorporating size-dependent effects and spatially varying thermal properties, providing new insights into thermal-mechanical coupling in micro-scale systems. Explicit formulas are derived for the inverse quality factor and frequency shifts, with the study comprehensively analyzing the influence of parameters such as beam thickness, aspect ratios, end constraints, relaxation constants, and fractional-order parameters. Novel findings reveal critical thickness ranges and phase-lag effects that govern energy dissipation and system dynamics. The results highlight the divergence from existing models, emphasizing the importance of non-local and fractional-order frameworks for accurately predicting damping and frequency behavior. Practical applications of the study include the optimization of micro-electromechanical systems (MEMS), nanoscale resonators, sensors, and energy-harvesting devices. By bridging theoretical advancements with tangible engineering solutions, this research provides a robust foundation for future exploration in thermal management and micro-scale system design, marking a significant contribution to the field. Graphical representations illustrate the effects of temperature discrepancy factors on damping and frequency shifts in non-simple micro-beams, offering a comprehensive understanding of the interaction between thermal and mechanical responses.

**Keywords:** Thermoviscoelastic, Relaxation time, Non-Fourier effect, Damping, Non-local, Heat source, Non-simple micro-beam, Inverse quality factor.

#### Introduction

Thermoviscoelasticity is the study that merges thermal, viscous, and elastic characteristics of materials to capture both their time-dependent deformation and the way they convert mechanical energy into heat. Damping refers to the inherent energy-dissipation mechanisms in viscoelastic materials. Under dynamic loading conditions, part of the

Department of Mathematics, Mahatma Gandhi College, Armori, Gadchiroli, India.

\*Corresponding Author: Gulshan Makkad, Department of Mathematics, Mahatma Gandhi College, Armori, Gadchiroli, India., E-Mail: gmakkad@gmail.com

**How to cite this article:** Makkad, G., Khalsa, L., and Varghese, V. (2025). Fractional thermoviscoelastic damping response in a non-simple micro-beam via DPL and KG nonlocality effect. The Scientific Temper, **16**(4):4151-4164.

Doi: 10.58414/SCIENTIFICTEMPER.2025.16.4.18

**Source of support:** Nil **Conflict of interest:** None.

mechanical energy is absorbed through the material's internal molecular friction and dissipated as heat.

Thermoviscoelasticity describes material behavior where deformation and heat transfer are interrelated, and damping refers to the dissipation of energy, often as heat, during oscillatory or vibrational motion. In thermoviscoelastic materials, the interaction between thermal and mechanical fields can result in damping, as energy is dissipated through heat generation during deformation. The deformation process in these materials may produce heat due to the material's viscous response and the coupling between thermal and elastic fields.

Thermoelastic damping is a critical factor in energy dissipation for vacuum-operated resonators that undergo transverse vibrations at room temperature. The material's thermal expansion coefficient causes thermoelastic coupling, inevitably leading to a temperature gradient along the beam's thickness. This temperature gradient drives irreversible heat flow, which increases entropy and ultimately converts the beam's elastic potential energy into thermal energy. Consequently, structures incorporating flexural vibration inherently exhibit thermoelastic damping.

**Received:** 16/03/2025 **Accepted:** 16/04/2025 **Published:** 25/04/2025

This damping is employed in aerospace, aircraft, and submarine designs to achieve high-precision performance and minimize unwanted vibrations and flutter (Bishop and Kinra, 1997). Thermoelastic damping adversely affects microbeam resonators, diminishing their sensitivity. Achieving a low level of thermoelastic damping is critical, as it signifies a high-quality factor in the resonators. Energy dissipation in micro-resonators occurs through two primary mechanisms: internal losses, which are mainly caused by thermoelastic damping, and external losses, including air damping and support loss. These external losses can be effectively reduced through precise manufacturing techniques and optimized structural designs (Lin, 2014).

Li et al. (2012) analyzed thermoelastic damping in circular and rectangular microplates with fully clamped and simply supported boundaries. Bostani and Mohammadi (2018) employed the Euler–Bernoulli beam theory in conjunction with the modified strain gradient theory, revealing significant differences in thermoelastic damping across the modified strain gradient, modified couple stress, and classical beam theories.

A notable approach for estimating thermoelastic damping in beams and plates is the complex frequency technique. Lifshitz and Roukes (2000) utilized the unidirectional coupled thermoelastic theory to derive a more accurate analytical expression for the inverse quality factor. Sun et al. (2006) explored the influence of thermoelastic coupling on damping in micro-beam resonators, employing generalized thermoelastic theory with relaxation time. Vahdat and Rezazadeh (2011) analyzed the impact of axial and residual stresses on thermoelastic damping in capacitive micro-beam resonators using twodimensional non-Fourier thermoelasticity theory. Guo (2013) utilized the generalized thermoelasticity theory for microbeams to derive an expression for thermoelastic damping. Hendou and Mohammadi (2014) analyzed the effects of geometric nonlinearity on thermoelastic damping in Euler-Bernoulli micro-beams. Borjalilou et al. (2019) applied the dual-phase-lag heat conduction model and the modified couple stress theory to predict thermoelastic damping in micro-beams at small scales. Gu et al. (2021) investigate the limitations of classical thermoelastic damping (TED) models in the design of micro/nano-devices, utilizing non-local strain gradient theory and dual-phase-lag heat conduction.

Mihailovich and MacDonald (1995) studied the mechanical loss in numerous micron-sized single-crystal silicon resonators operating in vacuum to identify the primary loss mechanism. Their investigation focused on three possible contributors to mechanical loss which includes doping-impurity losses, surface-related losses, and support-related losses. Zhang *et al.* (2003) analyzed the influence of air damping on the frequency response and quality factor of a micro-machined beam resonator. Zener

(1937) predicted the existence of the thermoelastic damping process and experimentally validated the core principles of the theory. Berry (1955) further conducted experiments on a-brass, which supported Zener's concept, measuring damping at room temperature as a function of frequency. Yasumura *et al.* (1999) observed thermoelastic damping in silicon nitride micro-resonators at room temperature, although their measurements were an order of magnitude smaller than Roszhardt's (1990) findings for thermoelastic damping in single-crystal silicon micro-resonators under similar conditions. Manolis and Beskos (1980) examined the effects of axial loads and damping on beam vibrations induced by rapid surface heating.

Although the connection between temperature and stress fields was disregarded, the effects of damping and axial loading were considered. Copper and Pilkey (2002) proposed a thermoelastic solution method for beams with arbitrary quasi-static temperature distributions that induce significant transverse normal and shear stresses. Previous studies have explored the influence of thermoelastic damping's size on the vibration frequency response of micro-resonators. Guo and Rogerson (2003) examined the size dependence of thermoelastic coupling in a doubly clamped elastic prism beam.

Lifshitz and Roukes (2000) conducted a study on thermoelastic damping in beams with rectangular crosssections, revealing that thermoelastic attenuation decreases with increasing size after the Debye peaks. However, the conclusions of both Guo and Rogerson (2003) and Lifshitz and Roukes (2000) were formulated using the classical Fourier heat conduction equation, without accounting for boundary conditions. Additionally, several notable non-Fourier-based models exist, including the single-phase lagging (SPL) model derived from Lord-Shulman's thermoelasticity theory (Lord et al. (1967), Heydarpour (2016)), the dual-phase lagging (DPL) model based on Tzou's thermoelasticity theory (Tzou 2015, Othman et al. 2017), the three-phase lagging (TPL) model rooted in Choudhuri's thermoelasticity theory [Kumar (2018), Choudhuri(2007)], and the Green-Naghdi thermoelasticity theory [Marin(2017), Wang(2016)]. Abbas (2015) examines thermoelastic interactions in functionally graded materials (FGMs) subjected to thermal shock, utilizing the fractionalorder three-phase lag model to formulate governing equations. Carrera et al. (2015) investigate the influence of two-temperature effects on a microbeam under ramp-type heating, employing generalized thermoelasticity theory and a relaxation time model to illustrate behavior across the microbeam's thickness. Mondal and Sur (2025) study thermoelastic interactions in a permeating rod, emphasizing non-Fourier heat conduction in thermomass gas flow within the framework of generalized thermoelasticity theory.

Kalkal et al. (2020) examine plane wave reflection in a rotating thermoelastic medium, focusing on four coupled

plane waves and demonstrating that the modulus of energy ratios equals unity at every incidence angle. Wang (2020) examines thermoelastic damping in micro-beams, highlighting the accuracy of memory-dependent heat conduction over classical models for small-scale resonators. Zhou (2021) explores thermoelastic damping (TED) and frequency shift in micro/nano-ring resonators, emphasizing the effects of heat-conduction dimension (HCD) and dual-phase-lagging (DPL) non-Fourier heat conduction. Key findings reveal that geometrical parameters, material properties, and DPL effects significantly influence TED and frequency shifts. Gu (2021) develops a scale-aware theoretical model for thermoelastic damping (TED) in micro-beam resonators, highlighting the effects of small-scale parameters like nonlocality, length scale, and slenderness ratio. It presents a size-dependent Q-factor formula and compares it with classical models, aiming to improve the design of micro/nanoscale devices. Singh (2007) analyzes the governing equations of Lord-Shulman's theory for a two-dimensional, homogeneous, isotropic generalized thermoelastic half-space with voids, focusing on compressional and shear wave reflection phenomena.

Recent studies include the work of Abouelregal et al. (2024), who introduced a novel viscoelastic heat transfer model. This model incorporates a memory-based derivative with the Moore-Gibson-Thomson equation to analyze the properties and behavior of polymers under external stresses. Makkad et al. (2025) proposed an innovative thermoviscoelasticity model based on fractional calculus to examine the thermal and mechanical characteristics of a non-simple nanobeam subjected to ramp-type heat loading. Similarly, Chandel et al. (2024) investigated thermoelastic heat transfer in a spherically symmetric sphere under point impulsive thermal loading, employing memory-dependent derivatives to predict the behavior of nanostructures. Zhang's (2016) study models thermoelastic damping (TED) in micro- and nanomechanical beam resonators, emphasizing size effects such as phonon mean-free path and relaxation time. Results show non-local effects are negligible at small scales, while size effects significantly impact energy dissipation, especially at submicron levels. Kakhki et al. (2015) provide an analytical framework for analyzing thermoelastic damping (TED) and dynamic behavior in MEMS microbeam resonators under diverse boundary conditions. It leverages modified coupled stress theory and Laplace transform techniques, offering an accurate alternative to numerical methods. Guo et al. (2012) examine thermoelastic damping (TED) in micro-beam resonators using the dualphase-lagging (DPL) model, revealing that nanoscale TED can surpass traditional models like Lifshitz-Roukes' and Zener's approximations. It highlights the impact of thermal relaxation constants and their ratio on TED behavior, offering insights into nanoscale resonator design.

Advanced numerical techniques, such as the finite element method (FEM), have been adapted to include thermoviscoelastic phenomena by integrating mechanical displacement and heat flow conservation equations. This adaptation is essential because the heat generated during viscoelastic deformation influences the temperature field and subsequently alters material behavior. Building upon these foundational concepts, current research in thermoviscoelasticity delves into advanced models such as those employing fractional calculus or incorporating nonlocal effects to capture the intricate behaviors of materials at micro and nanoscales. These cutting-edge studies aim to enhance predictive models for damping characteristics under highly variable environmental conditions, ultimately contributing to the development of more resilient and efficient materials and structures.

While significant research has been conducted on thermoelastic damping in micro-beam resonators, a notable gap persists in applying fractional calculus and dual-phase-lag theory. Current studies predominantly rely on classical and modified Fourier-based models, which inadequately account for thermal relaxation effects and other critical factors. This research seeks to bridge this gap by introducing a fractional thermoviscoelastic damping analysis for non-simple micro-beams within the framework of dual-phase-lag theory. The inclusion of the dual-phaselag thermal conduction model, along with a non-uniform internal heat source, offers a novel framework to analyze real-world heat transfer mechanisms and their influence on micro-beams. The research derives an explicit formula to calculate the inverse quality factor and frequency shift, enabling precise characterization of these parameters. Furthermore, it thoroughly examines how damping behavior varies with different aspect ratios and boundary conditions, emphasizing the role of end constraints and aspect ratios in shaping both damping and frequency shifts.

This research investigates the interplay between frequency shifts and damping in a nanoscale microbeam. A novel non-simple model is introduced, incorporating temperature discrepancy factors to capture the coupling between heat and elastic deformations, facilitating the derivation of explicit damping formulas. The study examines the inverse quality factor through graphical representations and illustrations, deriving explicit expressions for frequency shift, attenuation, and the inverse quality factor.

The paper is structured as follows: Section 2 outlines the mathematical framework for the governing equations of non-local Klein-Gordon elasticity theory. Section 3 discusses the practical considerations of heat conduction and the thermoelastic field. Section 4 focuses on deriving analytical solutions for temperature distribution and associated stress, highlighting the thermal effects on damping and frequency shifts. Section 5 presents parametric analyses and numerical results, while Section 6 concludes the study.

# Mathematical modeling and the fundamental equation

The non-local Klein-Gordon elasticity theory

According to Eringen's non-local elasticity theory [Eringen (1983)], the stress tensor at a given point x within an elastic body is influenced by the strain tensors at all other points in the body. Utilizing experimental findings on phonon dispersion and the atomic theory of lattice dynamics, the non-local stress tensor  $\sigma$  at position x can be formulated to reflect these interactions comprehensively as

$$\sigma(x) = \iiint_{v} K(|x'-x|,\zeta)t(x')dv, \tag{1}$$

where the kernel function  $K(|x'-x|,\zeta)$  represents the non-local modulus, where |x'-x| is the Euclidean distance and  $\zeta$  is a material constant determined by both internal and external characteristic lengths. Additionally, the generalized Hooke's law defines the classical (local) stress tensor at point x', denoted as t(x'). Given the complexity of solving elasticity problems through the integral constitutive relation in Eq. (1), other challenges are often addressed by employing an equivalent differential form of the integral constitutive relation. The differential form of Klein–Gordon non-local constitutive relations for an elastic body described in [Eringen (1983), Singh(2024)], is formulated as

$$(1 - \mu \nabla^2 + \tau^2 \partial_t^2) \sigma = t, \tag{2}$$

where  $\mu$  represents the non-local parameter given by

$$\mu = (\zeta l)^2 \text{ with } \zeta = \frac{e_0 a}{l},$$
 (3)

where a and l stand for the internal and external characteristic lengths, respectively, and  $e_0$  is a material constant. Given the thermoelastic constitutive relationships between the kinematic parameters and the local stresses, Eq. (2) can be expressed as

$$(1 - \mu \nabla^2 + \tau^2 \partial_t^2) \sigma = \frac{E}{(1 + \nu)(1 - 2\nu)} [\nu \varepsilon_{mm} I + (1 - 2\nu) \varepsilon - (1 + \nu) \alpha_0 \theta I], \quad (4)$$

where the identity and strain tensors are denoted by I and  $\varepsilon$ , respectively.

The strain tensor components  $\varepsilon$  are acquired using

$$\varepsilon_{ij} = \frac{1}{2} \left( \frac{\partial u_i}{\partial x_j} + \frac{\partial u_j}{\partial x_i} \right), \tag{5}$$

where  $u_i$  represents the components of the displacement vector u.

The strain tensor  $\varepsilon$  can be expressed in relation to the non-local stress tensor  $\sigma$  and the temperature increment  $\theta$ , derived using Eq. (4) as

$$\varepsilon = \frac{1}{E} [(1+\nu)(1-\mu\nabla^2 + \tau^2\hat{\sigma}_t^2)\sigma - \nu(1-\mu\nabla^2 + \tau^2\hat{\sigma}_t^2)\sigma_{mm}I] + \alpha_0\theta I,$$
(6)

# Non-simple dual-phase fractional heat conduction equation

In a thin micro-beam, the temperature gradient along the x-direction is insignificant compared to that along the z-direction (Lifshitz and Roukes, 2000). The energy equation given by Biot (1956) is

$$\rho C_{\nu} \frac{\partial T}{\partial t} - Q' = -\nabla \cdot q. \tag{7}$$

where Q' is an internal heat source.

To microscopically analyze the microstructural interactions in solid heat conductors, the temperature gradient  $\tau_T$  and heat flux vector  $\tau_q$  were translated into a dual-phase-lag model with delay time translation by Tzou (1995) as

$$q(t+\tau_{a}) = -k \nabla \Phi(t+\tau_{T}). \tag{8}$$

By using Taylor's series to expand both sides of Eq. (8) about the fractional order derivatives and keeping terms up to the  $2\alpha$  order in both phase-lags, one can derive

$$\left(1 + \frac{\tau_q^{\alpha}}{\alpha!} \frac{\partial^{\alpha}}{\partial t^{\alpha}} + \frac{\tau_q^{2\alpha}}{(2\alpha)!} \frac{\partial^{2\alpha}}{\partial t^{2\alpha}}\right) q = -k \left(1 + \frac{\tau_T^{\alpha}}{\alpha!} \frac{\partial^{\alpha}}{\partial t^{\alpha}} + \frac{\tau_T^{2\alpha}}{(2\alpha)!} \frac{\partial^{2\alpha}}{\partial t^{2\alpha}}\right) \nabla \Phi, \tag{9}$$

in which  $\alpha \in [0,1]$ .

Using Eq. (7) and application of the divergence operator on both sides of Eq. (9) yields

$$\left(1 + \frac{\tau_q^{\alpha}}{\alpha!} \frac{\partial^{\alpha}}{\partial t^{\alpha}} + \frac{\tau_q^{2\alpha}}{(2\alpha)!} \frac{\partial^{2\alpha}}{\partial t^{2\alpha}}\right) \left(\rho C_v \frac{\partial T}{\partial t} - Q'\right) = k \left(1 + \frac{\tau_T^{\alpha}}{\alpha!} \frac{\partial^{\alpha}}{\partial t^{\alpha}} + \frac{\tau_T^{2\alpha}}{(2\alpha)!} \frac{\partial^{2\alpha}}{\partial t^{2\alpha}}\right) \nabla^2 \Phi.$$
(10)

However, Quintanilla (2008) noted that if the energy equation provided by

$$-\nabla q(t) = c\,\dot{\Phi}(t),\tag{11}$$

and the heat conduction Eq. (10) is coupled, then the elements of a point spectrum can always be rearranged in such a way that the resulting equation's real part is close to infinity. This demonstrates the instability and ill-posedness of Tzou's proposed heat conduction model. As a result, Eq. (10) for heat conduction is unstable and ill-posed. Within the framework of two-temperature theory, Quintanilla (2008) demonstrated that the dual-phase-lag heat conduction Eq. (10) can be made well-posed and stable. In this context, Chen and Gurtin (1968) proposed categorizing real materials into simple and non-simple types by considering two distinct temperatures: conductive and thermodynamic. These temperatures are interrelated through

$$\Phi = (1 + \wp \nabla^2) T, \, \wp > 0. \tag{12}$$

In a simple medium, the thermodynamic temperature  $\Phi$  and the conductive temperature T are identical. However, in a non-simple material, these temperatures differ. Consequently, as a limiting case,  $\wp \to 0$ ,  $\Phi \to T$ , the classical one-temperature theory (1TT), is retrieved.

Thus, for a non-simple medium, Eq. (10) can be written as

$$D_{q}\left(\frac{\partial T}{\partial t} - \frac{Q'}{\rho C_{v}}\right) = \kappa \left(1 + \frac{\wp}{\kappa} \frac{\partial}{\partial t}\right) D_{T} \nabla^{2} T, \tag{13}$$

where

$$D_{q} = 1 + \frac{\tau_{q}^{\alpha}}{\alpha!} \frac{\partial^{\alpha}}{\partial t^{\alpha}} + \frac{\tau_{q}^{2\alpha}}{(2\alpha)!} \frac{\partial^{2\alpha}}{\partial t^{2\alpha}}, \quad D_{T} = 1 + \frac{\tau_{T}^{\alpha}}{\alpha!} \frac{\partial^{\alpha}}{\partial t^{\alpha}} + \frac{\tau_{T}^{2\alpha}}{(2\alpha)!} \frac{\partial^{2\alpha}}{\partial t^{2\alpha}}. \quad (14)$$

In the above, the Laplacian operator has been taken as  $\nabla^2 = \frac{\partial^2}{\partial x^2} + \frac{\partial^2}{\partial z^2}$ . Eq. (10) represents the fractional thermoviscoelastic heat conduction equation, formulated within the dual-phase-lag framework and incorporating the principles of two-temperature theory.

## Fundamental equations of the Kelvin-Voigt model

The Kelvin-Voigt (K-V) model is a widely recognized macroscopic mechanical framework used to describe the viscoelastic behavior of materials. This model captures the phenomenon of delayed elastic response to applied stress, where the deformation exhibits time-dependent yet reversible characteristics. The practical implications of the interplay between mechanical and thermal forces in solids are prominent across various domains, including astronautics, aeronautics, high-energy particle accelerators, and atomic reactors. To begin, we consider a homogeneous, isotropic, thermally conducting thermoviscoelastic solid of the Kelvin-Voigt type, initially at an undeformed state and a uniform temperature  $T_0$ . The full set of differential equations of thermoviscoelasticity (2000) is composed if there are no body forces, be summed up as follows:

The equation of motion takes the form

$$\mu u_{i,j} + (\lambda + \mu) u_{j,j} = \rho \frac{\partial^2 u_i}{\partial t^2} + \beta T_{,i}.$$
 (15)

The constitutive equations have the form

$$(1 - \mu \nabla^2 + \tau^2 \partial_t^2) \sigma_{ii} = 2\mu e_{ii} + (\lambda e_{kk} - \beta T) \delta_{ii}. \tag{16}$$

The parameters  $\lambda$ ,  $\mu$  and  $\beta$  are expressed as

$$\lambda = \lambda_0 \left( 1 + \alpha_1 \frac{\partial}{\partial t} \right), \mu = \mu_0 \left( 1 + \alpha_1 \frac{\partial}{\partial t} \right), \beta = \beta_0 \left( 1 + \beta_1 \frac{\partial}{\partial t} \right),$$

$$\beta_0 = (3\lambda_0 + 2\mu_0)\alpha_1, \beta_1 = (3\lambda_0\alpha_1 + 2\mu_0\alpha_2)\alpha_1 / \beta_0.$$
(17)

## Formulation of the physical problem

The formulation of the physical problem introduces a novel approach to analyzing viscothermoelastic micro-scale beams by integrating the Kelvin-Voigt viscoelastic model with the classical Euler-Bernoulli beam theory (EBBT). This combination offers a comprehensive framework for studying the coupled thermal and mechanical behavior at micro-scale levels, emphasizing size-dependent effects and thermal relaxation phenomena. By focusing exclusively on transverse movement along the z-axis, the study simplifies the analysis while capturing the essential bending behavior of the beam, where any plane cross-section remains orthogonal to the neutral surface after bending. The neutral surface, which remains unstressed during bending, serves as a reference for understanding deformation and stress distribution. Incorporating viscoelasticity allows for the consideration of time-dependent mechanical responses such as creep and stress relaxation, while thermoelastic effects enable exploration of energy dissipation mechanisms like thermoelastic damping. This problem formulation provides critical insights into thermal-mechanical coupling in micro-scale beams, laying the groundwork for optimizing micro-electromechanical systems (MEMS) such as sensors and actuators.

We are studying a viscothermoelastic micro-scale beam with dimensions L, h, and b, as illustrated in Fig. 1 for the Kelvin-Voigt type model. When the thickness and width directions align with y and z – axes, respectively, the structure occupies the domain specified by  $0 \le x \le L, -b \le 2y \le b$  and

Consequently, the displacement components are expected to align with the principles of the Euler-Bernoulli Beam Theory (EBBT) as

$$u = -z\frac{\partial w}{\partial x}, \quad v = 0, \quad w(x, y, z, t) = w(x, t). \tag{18}$$

Substitution of Eq. (18) into Eq. (5), one obtains

$$\varepsilon_{xx} = -z \frac{\partial^2 w(x,t)}{\partial x^2}.$$
 (18a)

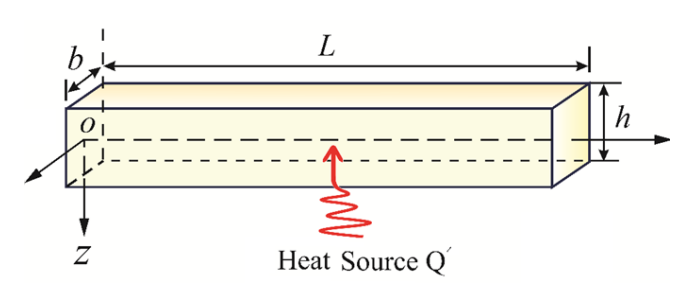


Figure 1: Configuration of the thermoviscoelastic micro-beam

With the displacement components as indicated in Eq. (18), the constitutive equation of the one-dimensional version in the presence of temperature can be expressed as

$$(1 - \mu \nabla^2 + \tau^2 \partial_t^2) \sigma_{xx} = -zE \frac{\partial^2 w(x, t)}{\partial x^2} - E\alpha_t T, \tag{19}$$

in which  $\sigma_{xx}$  is the constitutive equation reduced to the one-dimensional equation as

$$\sigma_{xx} = (\lambda + 2\mu) \frac{\partial u}{\partial x} - \beta T. \tag{20}$$

Also, Eq. (20), using Eq. (17) may be expressed as

$$\sigma_{xx} = \left(1 + \alpha_1 \frac{\partial}{\partial t}\right) \left[ (\lambda_0 + 2\mu_0) \frac{\partial u}{\partial x} \right] - \beta_0 \left(1 + \beta_1 \frac{\partial}{\partial t}\right) T. \tag{21}$$

Low-amplitude bending vibrations in the beam cause deformation consistent with the linear Euler-Bernoulli theory's assumptions. The widely accepted Euler-Bernoulli assumption (Boley, 1972) asserts that, during bending, any plane cross-section of the beam that was originally perpendicular to its axis retains its flatness and remains orthogonal to the neutral surface. At this stage, the bending moment formula can be obtained by replacing the integral component of Eq. (22) given below, with Eq. (21) as

$$M(x,t) = b \int_{-h/2}^{h/2} z \sigma_{xx} dz = -\left(EI \frac{\partial^2 w}{\partial x^2} + M_T\right), \tag{22}$$

and

$$M_T = bE \int_{-h/2}^{h/2} \alpha_t T(x, z, t) z dz.$$
 (23)

The governing equation of motion undergoing free flexural vibration is

$$\frac{\partial^2 M}{\partial x^2} = \rho A \frac{\partial^2 w}{\partial t^2}.$$
 (24)

The governing equation describing the beam's dynamic behavior can be formulated by integrating Eq. (24) into Eq. (23), resulting in the following expression

$$EI\frac{\partial^4 w}{\partial x^4} + (1 - \mu \nabla^2 + \tau^2 \partial_t^2) \rho A \frac{\partial^2 w}{\partial t^2} + \frac{\partial^2 M_T}{\partial x^2} = 0,$$
 (25)

subjected to the boundary conditions

$$w\Big|_{t=0} = 0, \frac{\partial w}{\partial t}\Big|_{t=0} = 0, \tag{26}$$

$$w\big|_{x=0} = 0, w\big|_{x=a_1} = 0,$$
 (27)

$$\left. \frac{\partial^2 w}{\partial x^2} \right|_{x=0} = 0, \left. \frac{\partial^2 w}{\partial x^2} \right|_{x=a_1} = 0.$$
(28)

Taking into account the volume strain as  $-z \partial^2 w / \partial x^2$ , as described in Eq. (18), Eq. (13) can be adapted for a non-simple medium as

$$D_{q}\left(\frac{\partial T}{\partial t} - \frac{Q'}{\rho C_{v}} - \frac{z\Delta_{E}}{\alpha_{t}} \frac{\partial^{2} w}{\partial x^{2}}\right) = \kappa \left(1 + \frac{\wp}{\kappa} \frac{\partial}{\partial t}\right) D_{T} \nabla^{2} T.$$
 (29)

In this case, the relaxation strength of the Youngs modulus is represented by  $\Delta_E = T_0 E \alpha_t^2 / \rho C_v$ , also known as the Zener modulus (5). It should be mentioned that there are no temperature gradients in the perpendicular direction. However, compared to gradients along the beam's axis, thermal gradients situated perpendicularly inside the cross-section's plane are much higher. We ignore the terms  $\partial^2/\partial x^2$ , and replace  $\nabla^2$  by  $\partial^2/\partial z^2$  (Zhang and Li, 1972).

$$D_{q} \left( \frac{\partial T}{\partial t} - \frac{Q'}{\rho C_{v}} - \frac{z \Delta_{E}}{\alpha_{t}} \frac{\partial^{2} w}{\partial x^{2}} \right) = \kappa \left( 1 + \frac{\wp}{\kappa} \frac{\partial}{\partial t} \right) D_{T} \frac{\partial^{2} T}{\partial z^{2}}. \tag{30}$$

Additionally, we assume that there is no heat transmission between the upper and lower sides of the beam as

$$\frac{\partial T}{\partial z}\Big|_{z=0} = \frac{\partial T}{\partial z}\Big|_{z=0} = 0, t > 0.$$
 (31)

#### Solution of the physical problem

Dimensionless parameters

To transform the dimensionless system of governing equations, the subsequent non-dimensional parameters are introduced as

$$\tilde{x} = x/L, \tilde{w} = w/h, \tilde{z} = z/h, \tilde{h} = h/L, (\tilde{t}, \tilde{\tau}_q, \tilde{\tau}_T) = (c/L)(t, \tau_q, \tau_T),$$

$$c^2 = E/\rho, \tilde{T} = T/T_c, \tilde{\psi} = (c/L)\omega, \tilde{O}' = (L/T_cc)O', \tilde{M}_T = (\beta L/\rho h^2 c^2)M_T.$$
(32)

Utilizing Eq. (32), governing Eq. (30), Eq. (25), and the boundary conditions (26)-(28) gives the dimensionless form of this model, which, by omitting the tilde sign for the sake of brevity, can be simplified as

$$D_{q} \left( \frac{\partial T}{\partial t} - \frac{Q'}{\rho C} - \frac{zh^{2}L\Delta_{E}}{cT_{0}\alpha_{e}} \frac{\partial^{2}w}{\partial x^{2}} \right) = \frac{\kappa}{Lch^{2}} \left( 1 + \frac{\wp}{\kappa} \frac{\partial}{\partial t} \right) D_{T} \frac{\partial^{2}T}{\partial z^{2}}, \quad (33)$$

$$L^{2} \frac{\partial^{2} w}{\partial t^{2}} + \frac{1}{b} \frac{\partial^{2} M_{T}}{\partial x^{2}} = -\frac{h^{2}}{12} \frac{\partial^{4} w}{\partial x^{4}},$$
(34)

$$w\big|_{t=0} = 0, \frac{\partial w}{\partial t}\bigg|_{t=0} = 0, \tag{35}$$

$$w\big|_{x=0} = 0, w\big|_{x=a} = 0,$$
 (36)

$$\left. \frac{\partial^2 w}{\partial x^2} \right|_{x=0} = 0, \frac{\partial^2 w}{\partial x^2} \right|_{x=0} = 0, \tag{37}$$

$$u = -z \frac{\partial w(x,t)}{\partial x}.$$
 (38)

### Thermal effects on the damping and frequency shifts

The novelty of this study lies in its detailed exploration of thermal effects on damping and frequency shifts, as well as the incorporation of a non-uniform internal heat source to model real-world heat transfer phenomena.

By setting

$$\begin{cases}
T(x,z,t) \\
Q'(x,z,t) \\
w(x,t)
\end{cases} = \begin{cases}
\theta(x,z) \\
Q(x,z) \\
w^*(x)
\end{cases} e^{i\omega t},$$
(39)

the study effectively captures the dynamic interplay between thermal and mechanical responses in micro-scale systems. This approach allows for a precise analysis of how thermal relaxation and phase-lag parameters influence energy dissipation (damping) and frequency shifts in micro-beams.

#### Significance of internal heat source

The heat source  $Q(x,z) = x\cos k_i z$  is crucial in heat transfer due to its non-uniform heat generation distribution, which can mimic real-world phenomena and serve as a test function for analytical and numerical methods. Its linear variation along the x-direction can model situations where material properties or external influences affect the rate of heat generation with position. The  $\cos k_i z$  term introduces periodic modulation in the z-direction. In general, the significance of a heat source  $Q(x,z) = x\cos k_i z$  lies in its ability to capture the subtleties of both periodic and linear spatial fluctuations in heat generation. For heat transfer investigations, this dual feature provides a solid foundation for testing analytical methods and numerical models, while also aiding in the understanding of the inherent behavior of non-uniformly heated systems.

Physically, the inclusion of such a heat source is crucial for understanding and optimizing heat transfer in advanced engineering applications, such as micro-electromechanical systems (MEMS) and nanoscale devices. It enables the study of localized thermal effects, which are often critical in determining the performance and reliability of these systems.

#### Thermoviscoelastic damping solutions

We expect to find complex frequencies, wherein the presence of thermoelastic coupling effect, the real part

Re ( $_{\omega}$ ) gives the new eigenfrequencies of the beam, and the imaginary part  $|\text{Im}(_{\omega})|$  represents the attenuation of vibration amplitude. Next, the amount of thermoelastic damping will be determined by expressing it as the inverse of the quality factor, which is provided by

$$\mathbb{Q}^{-1} = 2 \left| \frac{\operatorname{Im}(\omega)}{\operatorname{Re}(\omega)} \right|, \tag{40}$$

which is the ratio of energy lost per radian; the factor of 2 is since the beam's mechanical energy is proportional to the square of its amplitude.

Substitution of Eq. (39) into Eq. (32) leads to

$$\frac{\kappa}{cLh^{2}}\left(1+\frac{\wp}{\kappa}\frac{\partial}{\partial t}\right)D_{T}\frac{\partial^{2}\theta}{\partial z^{2}}-D_{q}i\omega\theta=-\left(\frac{zh^{2}L\Delta_{E}}{cT_{0}\alpha_{t}}\frac{\partial^{2}w^{*}}{\partial x^{2}}+\frac{x\cos k_{t}z}{\rho C_{v}}\right)D_{q}.$$
 (41)

Under those assumptions, the general solution of the governing Eq. (41) can be obtained as

$$\theta = C_1 \cos(k_i z) + C_2 \sin(k_i z) - \left(\frac{zh^2 L \Delta_E}{cT_0 \alpha_i} \frac{\partial^2 w^*}{\partial x^2} + \frac{x \cos k_i z}{\rho C_v}\right) \frac{D_q}{B_0}, \quad (42)$$

where

$$k_i^2 = \frac{B_0}{A_0}, \quad A_0 = \frac{\kappa L}{ch^2} \left( 1 + \frac{\wp}{\kappa} \frac{\partial}{\partial t} \right) D_T, \quad B_0 = -D_q i \omega, \tag{43}$$

and the constants  $C_1$  and  $C_2$  can be obtained by the boundary conditions given below

$$\left. \frac{\partial \theta}{\partial z} \right|_{z=h/2} = \left. \frac{\partial \theta}{\partial z} \right|_{z=-h/2} = 0. \tag{44}$$

Also,

$$\frac{\partial \theta}{\partial z} = -C_1 k_i \sin(k_i z) + C_2 k_i \cos(k_i z) - \left(\frac{h^2 L \Delta_E}{c T_0 \alpha_i} \frac{\partial^2 w^*}{\partial x^2} - \frac{x k_i \sin k_i z}{\rho C_n}\right) \frac{D_q}{B_0}. \tag{45}$$

Using Eq. (44), from Eq. (45) one obtains

$$C_1 = \frac{D_q x}{B_0 \rho C_v}; \quad C_2 = \sec\left(k_i \frac{h}{2}\right) \frac{D_q}{B_0 k_i} \frac{h^2 L \Delta_E}{c T_0 \alpha_i} \frac{\partial^2 w^*}{\partial x^2}. \tag{46}$$

Thus, using Eq. (39) and (46), Eq. (42) becomes

$$T = \left\{ \frac{D_{q}x}{B_{0}\rho C_{v}} \cos(k_{i}z) + \sec\left(k_{i}\frac{h}{2}\right) \frac{D_{q}}{B_{0}k_{i}} \frac{h^{2}L\Delta_{E}}{cT_{0}\alpha_{t}} \frac{\partial^{2}w^{*}}{\partial x^{2}} \sin(k_{i}z) - \left(\frac{zh^{2}L\Delta_{E}}{cT_{0}\alpha_{t}} \frac{\partial^{2}w^{*}}{\partial x^{2}} + \frac{x\cos k_{i}z}{\rho C_{v}}\right) \frac{D_{q}}{B_{0}} \right\} e^{i\omega t}.$$

$$(47)$$

Now, using Eq. (22), the thermal moment is obtained as

$$M_{T} = be^{i\omega t} \frac{h^{2}LD_{q}\Delta_{E}}{B_{0}cT_{0}\alpha_{t}} \frac{\partial^{2}w^{*}}{\partial x^{2}} \left\{ -\frac{h}{k_{i}^{2}} + \frac{2}{k_{i}^{3}} \tan\left(k_{i}\frac{h}{2}\right) - \frac{h^{3}}{12} \right\}.$$
 (48)

Using Eq. (48), Eq. (24) can be obtained as

$$\frac{h^2}{12} \{ 1 - \Delta \Delta_E [1 - g(\omega)] \} \frac{\partial^4 w^*}{\partial x^4} - \frac{\omega^2 w^*}{c^2} = 0, \tag{49}$$

where

$$\Delta = \frac{12\beta\Lambda(D_q)h}{h^2k_i^2} , \Lambda(D_q) = \frac{D_qhL}{\rho c^3B_0T_0\alpha_i},$$
 (50)

and

$$g(\omega) = \frac{2}{hk} \tan\left(\frac{k_i h}{2}\right) + \frac{h^2 k_i^2}{12}.$$
 (51)

By solving Eq. (49), we obtain the thermoelastic vibration of the beam as,

$$w^* = P_1 \sin(px) + P_2 \cos(px) + P_3 \sinh(px) + P_4 \cosh(px), \tag{52}$$

where

$$p = \left(\frac{12\omega^2}{c^2 h^2 \left[1 - \Delta \Delta_E \left\{1 - g(\omega)\right\}\right]}\right)^{1/4},\tag{53}$$

and the coefficients  $P_1, P_2, P_3$ , and  $P_4$  are constants. To calculate the constants, we use the boundary conditions Eqs. (34)-(36) at the two beam ends.

The dispersion relationship between  $_{\omega}$  and  $p_{_{n}}$  is calculated as

$$\omega = p_n^2 \left( \frac{h^2}{12} \left[ 1 - \Delta \Delta_E \left\{ 1 - g(\omega) \right\} \right] \right)^{1/2}.$$
 (54)

We ignore higher-order terms  $\Delta_{\it E}^{\it 2}$  corrections and keep the first-order term.

Furthermore, when looking for an approximate solution, we can replace  $g(\omega)$  in the square root by  $g(\omega_0)$ . Furthermore, the dispersion relation as can be seen in Eq. (51) is expressed as

$$\omega = \omega_0 \left( 1 - \frac{\Delta \Delta_E \left\{ 1 - g(\omega_0) \right\}}{2} \right). \tag{55}$$

If we take  $\Delta_E = 0$  in Eq. (54), the equation can be rewritten as  $\omega_0 = p_n^2 (h^2/12)^{1/2}$ , n = 1, 2, ... As previously stated, the discovery makes it convenient to separate the real components and imaginary components, obtain the thermoelastic beam's eigenfrequencies, and compute the required attenuation coefficients

$$\operatorname{Re}(\omega) = \omega_0 \left( 1 - \frac{\Delta \Delta_E \left\{ 1 - \operatorname{Re}[g(\omega_0)] \right\}}{2} \right), \tag{56}$$

$$\operatorname{Im}(\omega) = \omega_0 \left( \frac{\Delta \Delta_E \left\{ \operatorname{Im}[g(\omega_0)] \right\}}{2} \right). \tag{57}$$

Further, we anticipate that the frequencies will be complex, with the real component  $\operatorname{Re}(\omega)$  supplying the new eigenfrequencies of non-simple circular nanobeams in the presence of thermoelastic coupling and the imaginary part  $|\operatorname{Im}(\omega)|$  providing vibration attenuation. In this case  $\Delta_E << 1$ , the thermoelastic damping can be described in terms of the inverse quality factor given by

$$\mathbb{Q}^{-1} = 2 \left| \frac{\operatorname{Im}(\omega)}{\operatorname{Re}(\omega)} \right| = \Delta \Delta_E \left| \operatorname{Im}[g(\omega_0)] \right|. \tag{58}$$

The definition of  $\mathbb Q$  in an electrical circuit is like that of definition (55). Like the electrical example,  $\mathbb Q$  typically varies with frequency in this case. The frequency shift brought on by thermoelastic damping is computed using the relation

$$\delta = \left| \frac{\operatorname{Re}(\omega) - \omega_0}{\omega_0} \right| = \left| \frac{\Delta \Delta_E \left\{ 1 - \operatorname{Re}[g(\omega_0)] \right\}}{2} \right|. \tag{59}$$

#### **Numerical Result and Discussion**

The solutions illustrated across various figures are found to fully satisfy the boundary conditions, as outlined below. In this section, the dependence of the thermoelastic damping is demonstrated using numerical calculations and an example. The material parameters of a silicon beam are listed in Table 1 (Wong, 2006).

We shall take into account the range of beam length  $a(1-100)\times 10^{-12}\,\mathrm{m}$  and an aspect ratio  $\wp/h=10$  for the nanoscale beam. In the picoseconds  $(1-100)\times 10^{-14}\,\mathrm{sec}$ , the initial time t will be taken into account. The beam length when  $\wp=1$ , and z=h/6 were used to prepare the figures.

# Impact of varying phase lags on thermoelastic damping and frequency shift

Figure 2 illustrates shows the variation in the thermoelastic damping  $Q^{-1}/\Delta_E$  along thickness h for varying temperature phase-lag  $\tau_T$  and for fixed heat flux phase lag  $\tau_q = 0.4$  with a given value of temperature discrepancy factor  $\wp$  and aspect ratio  $\wp/h = 10$ .

Table 1: Material properties of silicon.

Table 1. Material properties of silicon.		
Parameters	Value	Unit
Density $ ho$	2330	$kg / m^3$
Specific heat capacity $C_{\scriptscriptstyle  m V}$	$1.64 \times 10^6$	$J/m^3K$
Thermal expansion coefficient $lpha$	$2.60 \times 10^{-6}$	$K^{-1}$
Thermal conductivity $\kappa$	141.04	w / mK
Young's modulus ${\cal E}$	165	GPa
Poisson's ratio $\nu$	0.22	

It shows how the thermoelastic damping (TED) varies along the thickness of viscoelastic micro-scale beams under different temperature phase-lag  $\tau_{\scriptscriptstyle T}$  conditions. As the beam thickness increases, TED initially rises, peaks, and then decreases, showcasing the interplay between thermal and mechanical effects. The graph reveals that higher  $\tau_{\tau}$  values amplify thermal relaxation effects, leading to greater energy dissipation, as evidenced by increased inverse quality factor (Q<sup>-1</sup>). Additionally, the comparison between local and nonlocal models underscores the importance of considering size-dependent effects at micro-scales, with non-local models providing a more accurate representation of TED. A closer examination within the thickness range of 46-60  $\mu$ m highlights subtle variations in  $Q^{-1}/\Delta_E$ , offering critical insights into the influence of  $\tau_T$  on damping. These findings have practical implications, enabling engineers to optimize material and geometric properties for micro-scale beams by leveraging the impact of thermal relaxation constants and their ratios.

Figures 3 shows the variation in the thermoelastic damping  $Q^{-1}/\Delta_E$  along thickness h for varying heat flux  $\tau_a$  phase lag and for fixed temperature phase lag  $\tau_T = 0.4$  with a given value of temperature discrepancy factor  $\wp$  and aspect ratio  $\wp/h = 10$ . It also illustrates how thermoelastic damping (TED) varies along the thickness h of viscoelastic micro-scale beams for different heat flux phase-lag  $\tau_a$  values, while keeping the temperature phaselag constant. As the thickness increases, TED initially rises, peaks, and then decreases, reflecting the dynamic interplay between thermal and mechanical effects. Higher  $\tau_a$  values correspond to greater energy dissipation, as indicated by higher inverse quality factor (Q<sup>-1</sup>) values, and the peak damping shifts towards larger thicknesses. This behavior highlights the significant role of heat flux phase-lag in influencing thermal relaxation effects.

The graph also compares local (solid lines) and non-local (dashed lines) models, emphasizing the importance of size-dependent effects at micro-scales. Non-local models show distinct variations in TED, particularly in the zoomed-in thickness range of  $40-54~\mu m$ , where subtle differences between local and non-local effects become more apparent.

Figure 4 reveals the relationship between frequency shift  $\delta/\Delta E$  and beam thickness h for varying heat flux phase-lag  $\tau_q$ , with a fixed temperature discrepancy factor  $\wp$ , and aspect ratio  $\wp/h=10$ . Initially, for thicknesses up to 40  $\mu m$ , the frequency shift remains constant, indicating that the beam's thickness has negligible influence in this range. Beyond 40  $\mu m$ , the thickness begins to significantly affect the frequency shift, with the highest peak observed between 40  $\mu m$  and 60  $\mu m$ , particularly around 10  $\mu m$  within this range. This peak suggests a critical thickness where the interaction between thermal and mechanical effects is most pronounced, leading to maximum frequency shift.

Interestingly, as the thickness exceeds 60  $\mu m$ , the frequency shift starts to increase again, indicating a secondary influence of beam thickness on the system's dynamic behavior. This trend underscores the complex interplay between heat flux phase-lag and beam thickness, which governs the thermal-mechanical coupling in microscale systems. These findings are crucial for optimizing the design of micro-scale resonators, as they highlight the importance of selecting appropriate thicknesses to achieve desired frequency characteristics.

# Impact of varying values of L/h on thermoelastic damping and frequency shift

Figure 5 illustrates the variation of thermoelastic damping (TED)  $Q^{-1}/\Delta_E$  with beam thickness h for different values of the parameter L/h in the Dual-Phase-Lag (DPL) model.

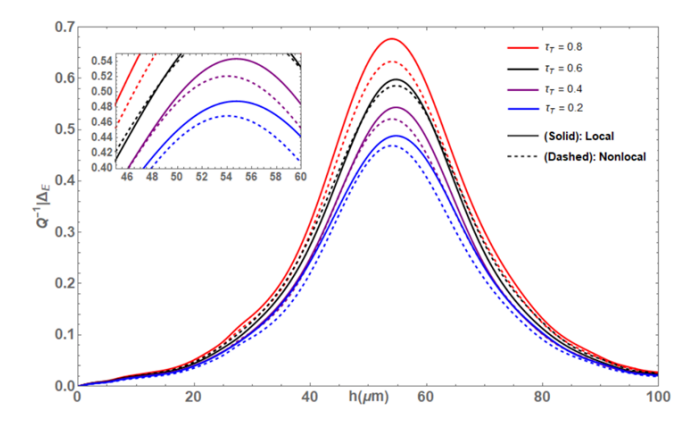
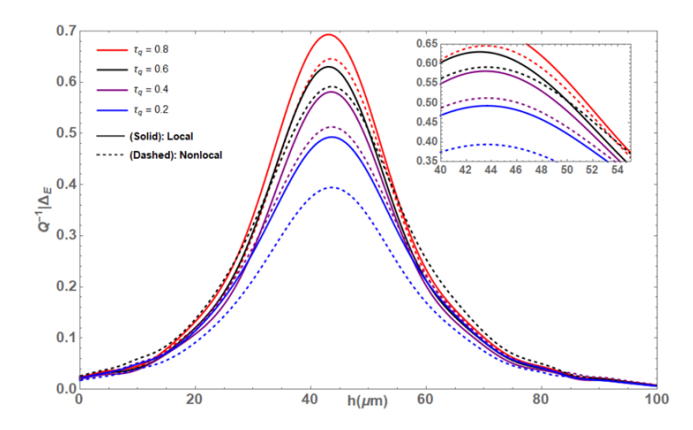
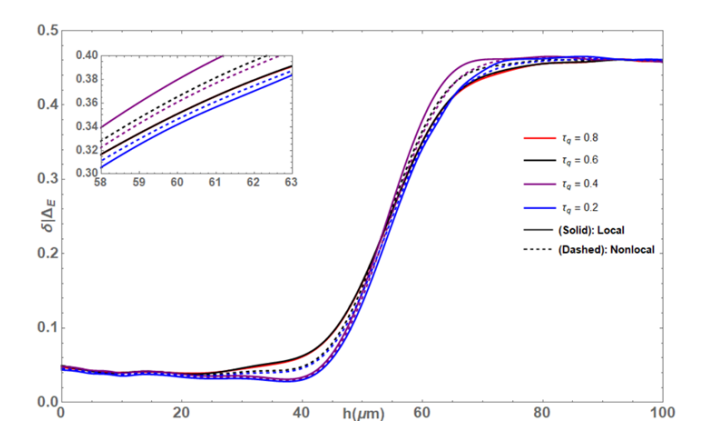


Figure 2: Variation of thermoelastic damping  $\,Q^{^{-1}}$  /  $\Delta_E$  with the beam thickness h for varying  $\,\tau_T$ 



**Figure 3:** Variation of thermoelastic damping  $Q^{-1}/\Delta_E$  with the beam thickness h for varying  $\tau_q$ 



**Figure 4:** Frequency shift  $\delta / \Delta E$  with the beam thickness h for varying heat flux  $\tau_a$ 

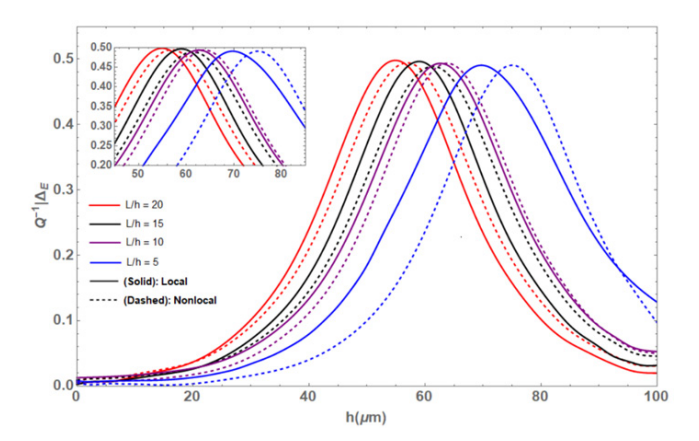
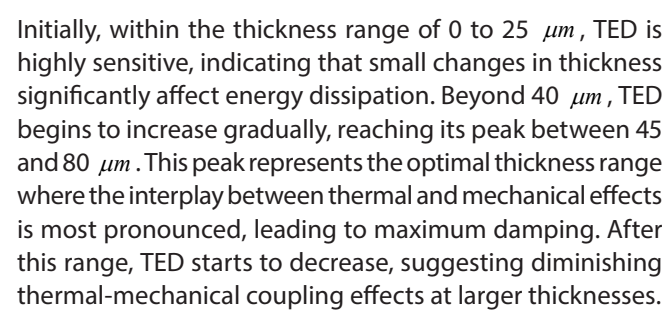


**Figure 5:** Variation of thermoelastic damping  $\,Q^{^{-1}}/\,\Delta_{^E}\,$  with the beam thickness h



The graph also highlights that damping increases with decreasing L/h, implying that smaller values of L/h enhance the influence of thermoelastic effects. This behavior underscores the importance of the parameter L/h in controlling energy-dissipation mechanisms in micro-scale systems. At other thicknesses, TED is negligible, indicating minimal energy loss due to thermoelastic effects. These findings are crucial for designing micro-scale resonators, as they provide insights into selecting appropriate thickness and L/h values to achieve desired damping characteristics.

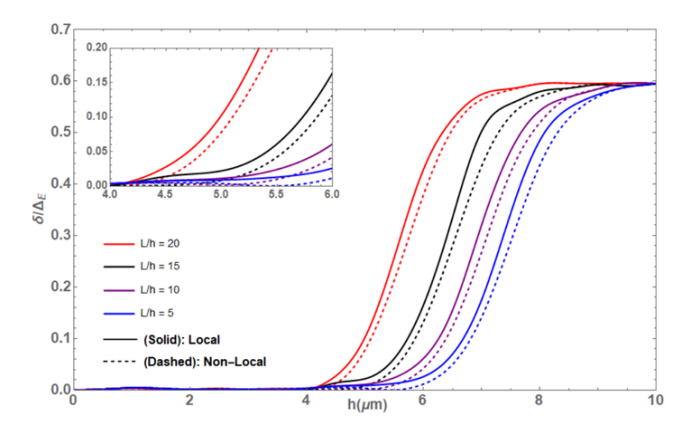


**Figure 6:** Frequency shift  $\delta / \Delta E$  with the beam thickness h for varied values of L/h

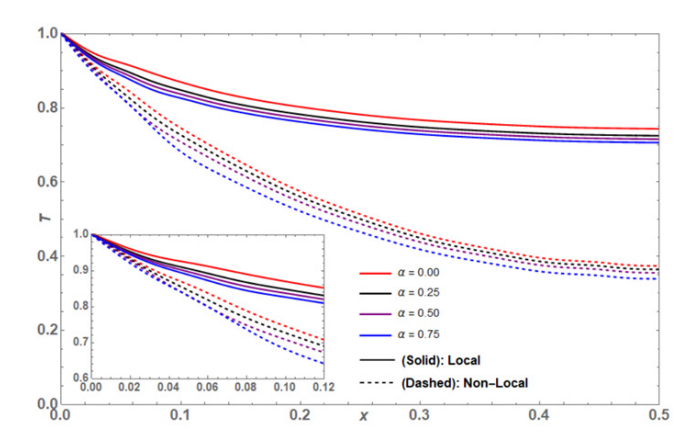


**Figure 7:** Effect of fractional order parameter  $\alpha$  on temperature T versus x

Figure 6 illustrates the frequency shift  $\delta/\Delta E$  as a function of beam thickness h for varied values of the ratio L/h. Initially, the frequency shift remains relatively stable for smaller thickness values, indicating minimal influence of L/h on the system's dynamic behavior in this range. As the thickness increases, the frequency shift begins to exhibit significant variations, with distinct peaks observed for different L/h values. These peaks suggest critical thickness ranges where the interaction between thermal and mechanical effects is most pronounced, leading to noticeable changes in frequency.

The comparison between local (solid lines) and non-local (dashed lines) models highlights the importance of size-dependent effects at micro-scales. Non-local models show more pronounced variations in frequency shift, particularly in the zoomed-in thickness range of 4–6  $\mu m$ , where subtle differences between local and non-local effects become evident. These findings underscore the role

of L/h in governing the dynamic behavior of micro-scale systems, offering valuable insights for optimizing the design of resonators and other mechanical components.

# Impact of fractional order parameter $\alpha$ on temperature

The graph in Figure 7 illustrates the temperature profiles T versus the spatial variable x for different values of the fractional order parameter  $\alpha$ , with a focus on the influence of the phase lag time  $\tau_T$  for the temperature gradient. As  $\alpha$  increases from 0.0 to 0.75, the temperature profiles exhibit greater changes, indicating that higher fractional order parameters amplify the thermal response in the system. This behavior highlights the significant role of fractional order in governing heat transfer dynamics.

The comparison between local and non-local models further emphasizes the importance of considering size-dependent effects in micro-scale systems. Non-local models show distinct variations in temperature profiles, particularly in the zoomed-in range of  $0 \le x \le 0.12$  where subtle differences between local and non-local effects become more apparent. These findings underscore the critical influence of fractional order parameters and phase lag times on temperature distribution, offering valuable insights for optimizing heat transfer models in advanced engineering applications.

Figure 8 illustrates the temperature variation T versus t for  $\tau_q = 3$ , and x = 3. The graph depicting the effect of the fractional order parameter  $\alpha$  on temperature T versus time t reveals significant insights into the thermal behavior of the system. As  $\alpha$  increases (from 0.0 to 0.75), the temperature rises more rapidly, reaches a higher peak, and then decreases more sharply. This indicates that higher fractional order parameters amplify the system's thermal response, making it more sensitive to external influences.

The local and non-local models show similar trends, but the non-local model generally predicts slightly higher

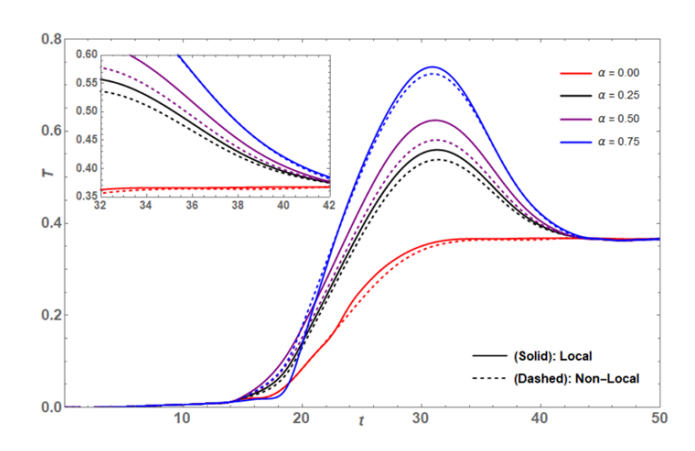


Figure 8: Effect of fractional order parameter  $\, lpha \,$  on temperature T  $\,$  versus t

temperatures, emphasizing the importance of size-dependent effects in micro-scale systems. The inset graph, which zooms in on a specific time range, highlights subtle variations in temperature behavior for different  $\alpha$  values, further underscoring the role of fractional order parameters in controlling the rate of temperature change and peak temperature.

These findings are crucial for applications requiring precise thermal management, as they demonstrate how adjusting  $\alpha$  can influence the system's thermal dynamics.

### Conclusion

This study investigates thermoelastic damping in microscale beams by combining the Euler-Bernoulli beam theory with a two-temperature thermoviscoelastic model. It incorporates non-Fourier effects and fractional-order parameters to provide a deeper understanding of the phenomenon. Several key conclusions emerge from the numerical results, highlighting the study's contributions to this field are as follows:

- The relaxation time of heat flux impacts the frequency shift and damping, though its effect on these parameters remains negligible. This aligns with the graphical analyses that show limited effects of heat flux phase-lag on TED and frequency shifts.
- The TED initially increases, peaks, and then decreases as the beam thickness increases. Critical thickness ranges, such as 46–60 μm for temperature phase-lags and 40–54 μm for heat flux phase-lags, exhibit the most pronounced damping effects (Figs. 2 and 3).
- Frequency shift remains constant for smaller thicknesses but shows significant variation for larger ones. Peak shifts occur between 40–60  $\mu$ m, highlighting critical ranges where thermal-mechanical interactions are most pronounced (Fig. 4).
- For beams with thicknesses of 0 μm to 100 μm, the non-Fourier effect plays a significant role in influencing both damping and frequency shift. The study emphasizes the critical role of non-Fourier effects within the Dual-Phase-Lag (DPL) thermal conduction model, as discussed in Figs. 5 and 6.
- TED increases with decreasing values of *L/h*, underscoring the critical role of this parameter in controlling energy dissipation mechanisms for micro-scale systems. Frequency shift remains stable at smaller thicknesses but exhibits distinct variations at larger ones. Peaks between 40–60 μm highlight optimal thickness ranges where thermal and mechanical interactions are most pronounced. These findings offer crucial insights for selecting appropriate thickness and *L/h*, values to optimize damping and frequency characteristics in micro-scale resonators (Figs. 5 and 6).
- Increasing the fractional order parameter  $\alpha$  amplifies

the system's thermal response, resulting in greater temperature variations both spatially (x-direction) and temporally (t-direction). This underscores its importance in governing heat transfer dynamics in micro-scale systems (Figs. 7 and 8).

- As  $\alpha$  increases, temperature profiles exhibit more pronounced changes, reflecting a stronger thermal response. This effect is particularly evident in the zoomed-in range, where non-local models capture size-dependent variations more accurately (Fig. 7). Larger  $\alpha$  values lead to a faster temperature rise, higher peak, and sharper decline over time, highlighting the sensitivity of thermal behavior to fractional order parameters (Fig. 8).
- Comparisons between local and non-local models underscore the importance of considering sizedependent phenomena in micro-scale systems for accurate predictions of damping and frequency behavior.
- The associated non-Fourier effects have a strong influence on the distribution and response history of the thermoviscoelastic fields. Damping can cause a temperature reduction and energy loss even in the absence of heat transmission to the surrounding environment through convection and radiation. This aligns with the exploration of TED and its coupling with thermal responses, as depicted in the abstract and graphical representations.
- By highlighting the crucial impact of numerous parameters and offering insightful information for upcoming research and applications in this area, the study adds to the body of knowledge on thermoelastic damping in viscoelastic micro-scale beams. This encapsulates the study's contributions and its significance for future research in this domain,
- Numerical results emphasize the sensitivity of thermoelastic damping to variations in temperature and heat flux phase-lag parameters, highlighting the dynamic interplay between thermal and mechanical effects.

Overall, this study presents a novel framework for analyzing thermoelastic damping (TED) in micro-scale beams by combining the Euler-Bernoulli beam theory with a two-temperature thermoviscoelastic model. Incorporating fractional-order parameters, non-Fourier effects, and the dual-phase-lag thermal conduction model with a non-uniform internal heat source, it provides a detailed understanding of the interaction between thermal and mechanical responses. While gaps remain in coupling effects and experimental validation, this research lays the foundation for advancements in MEMS, nanoscale devices, energy harvesting, and thermal management, contributing significantly to the field of micro-scale system design and analysis.

## Acknowledgments

I sincerely thank my supervisor and my co-author for their valuable guidance and support throughout this research.

#### **Conflict of Interest**

The author(s) declared no potential conflicts of interest with respect to the research, authorship and publication of this article.

#### References

- Abbas I. (2015). Generalized thermoelastic interaction in functional graded material with fractional order three-phase lag heat transfer, J. Cent. South Univ. Vol. 22, pp. 1606–1613. DOI: 10.1007/s11771-015-2677-5
- Abouelregal A., Marin M., Askar S. and Foul A. (2024). A modified mathematical model for thermo-viscous thermal conduction incorporating memory-based derivatives and the Moore–Gibson–Thomson equation, Continuum Mech. Thermodyn. Vol. 36, pp. 585–606. DOI: 10.1007/s00161-024-01284-6
- Berry B. (1955). Precise investigation of the theory of damping by transverse thermal currents, J. Appl. Phys. Vol. 26, pp. 1221–1224. DOI: 10.1063/1.1721877
- Biot M. (1956). Thermoelasticity and irreversible thermodynamics, J. Appl. Phys. Vol. 27, no. 3, pp. 240–253. DOI: 10.1063/1.1722351
- Bishop J. and Kinra V. (1997). Elastothermodynamic damping in laminated composites, Int. J. Solids Struct. Vol. 34, no. 9, pp. 1075–1092. DOI: 10.1016/S0020-7683(96)00085-6
- Boley B. (1972). Approximate analyses of thermally induced vibrations of beams and plates, J. Appl. Mech. Vol. 39, pp. 212–216. DOI: 10.1115/1.3422615
- Borjalilou V., Asghari M. and Bagheri E. (2019). Small-scale thermoelastic damping in micro-beams utilizing the modified couple stress theory and the dual-phase-lag heat conduction model, J. Therm. Stresses Vol. 42, no. 7, pp. 801–814. DOI: 10.1080/01495739.2019.1590168
- Bostani M. and Mohammadi A. (2018) Thermoelastic damping in microbeam resonators based on modified strain gradient elasticity and generalized thermoelasticity theories, Acta Mech. Vol. 229, no. 7, pp.173–192. DOI: 10.1007/s00707-017-1950-0
- Carrera E., Abouelregal A., Abbas, I. and Zenkour A. (2015). Vibrational Analysis for an Axially Moving Microbeam with Two Temperatures, J. Therm. Stresses. Vol. 38. no. 6, pp. 569-590. DOI: 10.1080/01495739.2015.1015837
- Chandel N., Khalsa L., Varghese V. and Yadav A. (2024). Non-local thermoelastic analysis of a spherically symmetric elastic sphere with memory effects, Mechanics of Advanced Materials and Structures (MAMS). Vol. 15, no. 1, pp. 1-13. DOI: 10.1080/15376494.2024.2422575
- Chen P. and Gurtin M. (1968). On a theory of heat conduction involving two temperatures, Z. Angew. Math. Phys. Vol. 19, pp. 559-577. DOI: 10.1007/BF01594969
- Choudhuri S. (2007). On a thermoelastic three-phase-lag model, J. Therm. Stresses Vol. 30, no. 3, pp. 231–238. DOI: 10.1080/01495730601130919
- Copper C. and Pilkey W. (2002). Thermoelasticity solutions for straight beams, J. Appl. Mech. Vol. 69, no. 3, pp. 224–229. DOI: 10.1115/1.1427340
- Eringen A. (1983). On differential equations of non-local elasticity

- and solutions of screw dislocation and surface waves, J. Appl. Phys. Vol. 54, pp. 4703-4710. DOI: 10.1063/1.332803
- Gu B., He T. and Ma Y. (2021). Thermoelastic damping analysis in micro-beam resonators considering non-local strain gradient based on dual-phase-lag model, Int. J. Heat Mass Transf. Vol. 180, pp. 121771. DOI: 10.1016/j.ijheatmasstransfer.2021.121771
- Gu B., He T. and Ma Y. (2021). Thermoelastic damping analysis in micro-beam resonators considering non-local strain gradient based on dual-phase-lag model, Int. J. Heat Mass Transf. Vol. 180. DOI: 10.1016/j.ijheatmasstransfer.2021.12177.
- Guo F. (2013). Thermo-elastic dissipation of microbeam resonators in the framework of generalized thermo-elasticity theory, J. Therm. Stresses. Vol. 36, no. 11, pp. 1156–1168. DOI: 10.1080/01495739.2013.818903
- Guo F. and Rogerson G. (2003). Thermoelastic coupling effect on a micro-machined beam machined beam resonator, Mech. Res. Commun. Vol. 30, pp. 513–518. DOI: 10.1016/S0093-6413(03)00061-2
- Guo F. L., Wang G. Q. and Rogerson G. A. (2012). Analysis of thermoelastic damping in micro- and nanomechanical resonators based on dual-phase-lagging generalized thermoelasticity theory, Int. J. Eng. Sci., Vol. 60, pp. 59-65. DOI: 10.1016/j.ijengsci.2012.04.007
- Hendou R. and Mohammadi A. (2014). Transient analysis of nonlinear Euler–Bernoulli micro-beam with thermoelastic damping via nonlinear normal modes, J. Sound Vib. Vol. 333, no. 23, pp. 6224–6236. DOI: 10.1016/j.jsv.2014.07.002
- Heydarpour Y. and Aghdam M. (2016). Transient analysis of rotating functionally graded truncated conical shells based on the Lord–Shulman model, Thin-Walled Struct. Vol. 104, pp. 168–184. DOI: 10.1016/j.tws.2016.03.016
- Kakhki E., Hosseini S. and Tahani M. (2015). An analytical solution for thermoelastic damping in a micro-beam based on generalized theory of thermoelasticity and modified couple stress theory, Appl. Math. Model. Vol. 40, no. 4, pp. 3164-3174. DOI: 10.1016/j.apm.2015.10.019
- Kalkal K., Sheoran D. and Deswal S. (2020). Reflection of plane waves in a non-local micropolar thermoelastic medium under the effect of rotation, Acta Mech. Vol. 231, pp. 2849–2866. DOI: 10.1007/s00707-020-02676-w
- Kumar R., Kumar R. and Kumar H. (2018). Effects of phaselag on thermoelastic damping in micromechanical resonators, J. Therm. Stresses. Vol. 41, no. 3, pp. 1–10. DOI: 10.1080/01495739.2018.1469061
- Li P., Fang Y. and Hu R. (2012). Thermoelastic damping in rectangular and circular microplate resonators, J. Sound Vib. Vol. 331, no. 3, pp. 721–733. DOI: 10.1016/j.jsv.2011.10.005
- Lifshitz R. and Roukes M. (2000). Thermoelastic damping in microand nanomechanical systems, Phys. Rev. B. Vol. 61, pp. 5600–5609. DOI: 10.1103/PhysRevB.61.5600
- Lin S. (2014). Analytical solutions for thermoelastic vibrations of beam resonators with viscous damping in non-Fourier model, Int. J. Mech. Sci. Vol. 87, pp. 26–35. DOI: 10.1016/j. ijmecsci.2014.05.026
- Lord H. and Shulman Y. (1967). A generalized dynamical theory of thermoelasticity, J. Mech. Phys. Solid. Vol. 15, no. 5, pp. 299–309. DOI: 10.1016/0022-5096(67)90024-5
- Makkad G., Khalsa L., Yadav A. and Varghese V. (2025). Non-local Fractional Thermoviscoelastic Bending Analysis of Nonsimple Nanobeam Under Ramp-Type Heating, J. Elast. Vol.

- 157, no. 28. DOI: 10.1007/s10659-025-10119-7
- Manolis G. and Beskos D. (1980). Thermally Induced vibrations of beam structures, Comput. Meth. Appl. Mech. Eng. Vol. 21, pp. 337–355. DOI: 10.1016/0045-7825(80)90101-2
- Marin M. and Ochsner A. (2017). The effect of a dipolar structure on the Holder stability in Green-Naghdi thermoelasticity, Contin. Mech. Thermodyn. Vol. 29, no. 6, pp. 1365-1374. DOI: 10.1007/s00161-017-0585-7
- Mihailovich R. and MacDonald N. (1995). Dissipation measurements of vacuum-operated single-crystal silicon microresonators, Sens. Actuators A: Phys. Vol. 50, no. 3, pp. 199–207. DOI: 10.1016/0924-4247(95)01080-7
- Mondal S. and Sur. A. (2025). Thermal waves based on the thermomass model due to mechanical damage with memory, Appl. Phys. A. Vol. 131, no. 4. DOI: 10.1007/s00339-024-08133-y
- Mukhopadhyay S. (2000). Effects of thermal relaxations on thermoviscoelastic interactions in an unbounded body with a spherical cavity subjected to a periodic loading on the boundary, J. Therm. Stresses. Vol. 23, pp. 675–684. DOI: 10.1080/01495730050130057
- Othman M., Abd-Elaziz E. (2017). Effect of rotation on a micropolar magneto-thermoelastic solid in dual-phase-lag model under the gravitational field, Microsyst. Technol. Vol. 23, no. 10, pp. 4979–4987. DOI: 10.1007/s00542-017-3295-y
- Quintanilla R. (2008). A well-posed problem for the dual -phase-lag heat conduction, J. Therm. Stresses. Vol. 31, no. 3, pp. 260–269. DOI: 10.1080/01495730701738272
- Roszhardt R. (1990). The effect of thermoelastic internal friction on the Q of micromachined silicon resonators, IEEE Solid State Sensor and Actuator Workshop, Hilton Head Island, SC, USA, pp. 13–16.
- Singh B. (2007). Wave propagation in a generalized thermoelastic material with voids, Appl. Math. Comput. Vol. 189, no. 1, pp. 698-709 . DOI: 10.1016/j.amc.2006.11.123
- Singh B. (2024). Wave Propagation in context of Moore– Gibson–Thompson Thermoelasticity with Klein–Gordon Nonlocality, Vietnam J. Mech. Vol. 46, no. 2, pp. 104 – 118. DOI: 10.15625/0866-7136/19728
- Sun Y., Fang D. and Soh A. (2006). Thermoelastic damping in micro-beam resonators, Int. J. Solids Struct. Vol. 43, no. 10, pp. 3213–3229. DOI: 10.1016/j.ijsolstr.2005.08.011
- Tzou D. (1995). A unified approach for heat conduction from macro-to micro-scales, J. Heat Transf. Vol. 117, pp. 8–16. DOI: 10.1115/1.2822329
- Tzou D. (2015). Macro-to Microscale Heat Transfer: The Lagging Behavior, Second ed., John Wiley and Sons, West Sussex. DOI: 10.1002/9781118818275.fmatter
- Vahdat A. and Rezazadeh G. (2011). Effects of axial and residual stresses on thermoelastic damping in capacitive micro-beam resonators, J. Franklin Inst. Vol. 348, no. 4, pp. 622–639. DOI: 10.1016/j.jfranklin.2011.01.007
- Wang Y., Liu D., Wang Q. and J. Zhou (2016). Problem of axisymmetric plane strain of generalized thermoelastic materials with variable thermal properties, Eur. J. Mech. Solid. Vol. 60, pp. 28–38 DOI: 10.1016/j.euromechsol.2016.06.001
- Wang Y., Zhang X. and Li X. (2020). Thermoelastic damping in a micro-beam based on the memory-dependent generalized thermoelasticity, Waves Random Complex Media, Vol. 32, pp. 1-18. DOI: 10.1080/17455030.2020.1865590

- Yasumura K., Stowe T., Kenny T. and Rugar D. (1999). Bull. Am. Phys. Soc. Vol. 44, no. 1, pp. 540.
- Zener C. (1937). Internal friction in solids. I. Theory of internal friction in reeds, Phys. Rev. Vol. 52, pp. 230–235. DOI: 10.1103/PhysRev.52.230
- Zhang C., Xu G. and Jiang Q. (2003). Analysis of the air-damping effect on a micromachined beam resonator, Math. Mech. Solids. Vol. 8, pp. 315–325. DOI: 10.1177/1081286503008003006
- Zhang H., Kim T., Choi G. and Cho H. (2016). Thermoelastic damping in micro- and nanomechanical beam resonators considering
- size effects, Int. J. Heat Mass Transf. Vol. 103, pp. 783-790. DOI: 10.1016/j.ijheatmasstransfer.2016.07.044
- Zhang X. and Li X. (2021). Hygrothermoelastic damping of beam resonators with non-Fourier and non-Fick effects, Thin Walled Struct. Vol. 168, pp. 108283. DOI: 10.1016/j. tws.2021.108283
- Zhou H. and Li P. (2021). Dual-phase-lagging thermoelastic damping and frequency shift of micro/nano-ring resonators with rectangular cross-section, Thin-Walled Structures, Vol. 159. DOI: 10.1016/j.tws.2020.107309